# Osteocyte culture in microfluidic devices

Chao Wei,[1,a)] Beiyuan Fan,[1,a)] Deyong Chen,[1] Chao Liu,[2] Yuanchen Wei,[1] Bo Huo,[3] Lidan You,[2,b)] Junbo Wang,[1,b)] and Jian Chen[1,b)]
[1]*State Key Laboratory of Transducer Technology, Institute of Electronics, Chinese Academy of Sciences, Beijing 100190, People's Republic of China*
[2]*Institute of Biomaterials and Biomedical Engineering, University of Toronto, Toronto, Ontario M5S 3G9, Canada*
[3]*School of Aerospace Engineering, Beijing Institute of Technology, Beijing 100081, People's Republic of China*

(Received 19 August 2014; accepted 28 December 2014; published online 26 January 2015)

This paper presents a microfluidic device (poly-dimethylsiloxane micro channels bonded with glass slides) enabling culture of MLO-Y4 osteocyte like cells. In this study, on-chip collagen coating, cell seeding and culture, as well as staining were demonstrated in a tubing-free manner where gravity was used as the driving force for liquid transportation. MLO-Y4 cells were cultured in microfluidic channels with and without collagen coating where cellular images in a time sequence were taken and analyzed, confirming the positive effect of collagen coating on phenotype maintaining of MLO-Y4 cells. The proliferating cell nuclear antigen based proliferation assay was used to study cellular proliferation, revealing a higher proliferation rate of MLO-Y4 cells seeded in microfluidic channels without collagen coating compared to the substrates coated with collagen. Furthermore, the effects of channel dimensions (variations in width and height) on the viability of MLO-Y4 cells were explored based on the Calcein-AM and propidium iodide based live/dead assay and the Hoechst 33258 based apoptosis assay, locating the correlation between the decrease in channel width or height and the decrease in cell viability. As a platform technology, this microfluidic device may function as a new cell culture model enabling studies of osteocytes. © *2015 Author(s). All article content, except where otherwise noted, is licensed under a Creative Commons Attribution 3.0 Unported License*. [http://dx.doi.org/10.1063/1.4905692]

## I. INTRODUCTION

Osteoporosis, a disease due to an imbalance of bone formation and desorption,[1,2] is a major public threat and has a devastating effect on people's lives, leading to painful fractures, disability, or deformity.[3–6] Due to limited understandings on the underlying mechanisms, current osteoporosis therapies cannot address this imbalance properly.[7]

Recent studies suggest a coordinating role of osteocytes (bone cells embedded in bone matrix) in bone metabolism by regulating activities of osteoblasts (bone formation cell) and osteoclasts (bone desorption cell),[8–12] which may shed new treatment strategies for osteoporosis. However, current studies of osteocytes are based on conventional cell culture,[13,14] which cannot recapitulate local *in vivo* microenvironments, due to its incapability to control the spatial/temporal distribution of cells and biomolecules.[15]

Microfluidics is the science and technology of manipulating and detecting fluids in the microscale.[16,17] Due to its dimensional comparison with biological cells and capabilities of defining local biophysical, biochemical, and physiological cues, microfluidics has been used to

[a)]C. Wei and B. Fan contributed equally to this work.
[b)]Authors to whom correspondence should be addressed. Electronic addresses: youlidan@mie.utoronto.ca; jbwang@mail.ie.ac.cn; and chenjian@mail.ie.ac.cn

 © Author(s) 2015

construct more *in vivo* like cell culture models,[18–20] enabling tumor,[21,22] neuron,[23] and vascular[24,25] studies. However, in the field of microfluidics based bone studies, preliminary demonstrations were focused to osteoblasts,[26–29] while no systematic study of on-chip culture of osteocytes has been demonstrated.

To address this issue, we proposed a microfluidic platform (Figure 1) for on-chip culture of osteocytes where collagen coating (Figures 1(a) and 1(b)), cell seeding and culture (Figures 1(c)–1(e)), as well as immunostaining (Figures 1(f)–1(h)) were conducted in a tubing-free manner. More specifically, the effects of surface modification (with or without collagen coating) on the proliferation and morphology of osteocytes cultured in microfluidic channels were investigated. Furthermore, the influence of channel dimensions (variations in width and height) on the cellular viability was studied. Meanwhile, as gravity was used as the driving force for cell loading and immunostaining, this platform does not need external pumps and tubes, which can be operated in biological labs with low access requirement.

## II. MATERIALS AND METHODS

### A. Materials

All the cell culture reagents including alpha modified essential medium (α-MEM), fetal bovine serum (FBS), calf serum (CS), penicillin and streptomycin (P/S), and phosphate-buffered saline solution (PBS) were purchased from Life Technologies. Materials required for device fabrication included SU-8 photoresist (MicroChem Corp.) and 184 silicone elastomer (Dow Corning Corp.). Collagen type I from rat tail (Sigma) was used for microfluidic channel coating. Materials for cell viability analysis included Calcein-AM (Santa Cruz) and propidium iodide (Sigma). Hoechst 33258 (Sigma) was used to analyze cell apoptosis. Materials for proliferating cell nuclear antigen (PCNA) immunostaining included 4% paraformaldehyde (Sigma), goat serum (Gibco), primary antibody (Abcom), and GTVision Detection System (Gene Technology). Materials for E11/gp38 immunostaining included 4% paraformaldehyde (Sigma), goat serum (Gibco), primary antibody podoplanin 8.1.1, and secondary antibody goat anti-Syrian hamster IgG-FITC (Santa Cruz).

### B. Cell culture

MLO-Y4 osteocyte like cells (gift from Dr. Linda Bonewald, University of Missouri-Kansas City) were cultured on collagen-coated flasks in α-MEM media supplemented with 2.5% FBS, 2.5% CS, and 1% P/S at 37 °C and 5% $CO_2$. Immediately prior to an experiment,

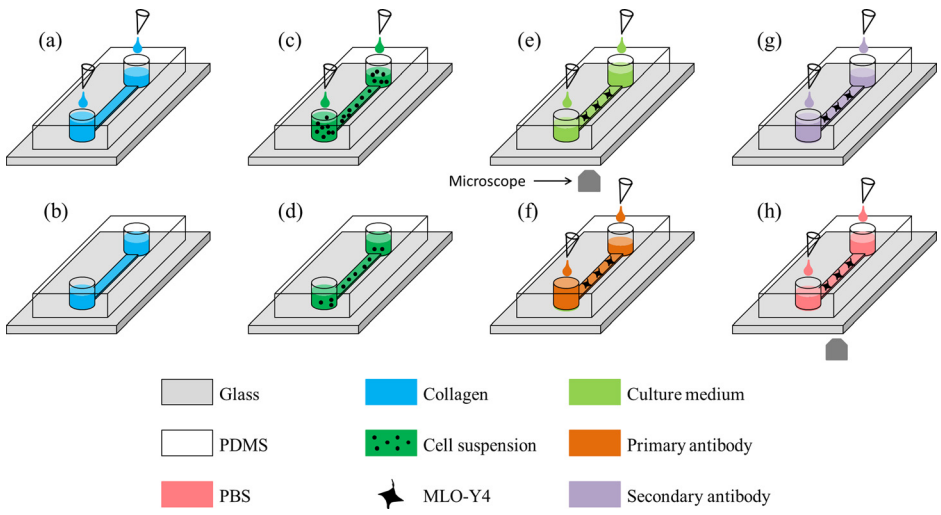


FIG. 1. Schematic of the tubing-free microfluidic platform for culture of MLO-Y4 cells where gravity was used for collagen coating ((a) and (b)), MLO-Y4 cell seeding, culture and medium replacement ((c)–(e)), as well as immunostaining ((f)–(h)).

MLO-Y4 cell suspensions were prepared with a concentration of $0.5 \times 10^6$ cells per ml. In this study, MLO-Y4 cell passage generations were between P5 and P14.

### C. Device design and fabrication

To investigate the effects of surface modification on osteocyte proliferation and morphology, microfluidic devices with default channel dimensions of 10.00 L × 0.80 W × 0.10 H (mm) were used. Meanwhile, microfluidic devices with variations in channel width (0.80 vs. 0.20 mm) and height (0.10 vs. 0.02 mm) were used to explore the effects of channel dimensions on cellular viabilities. Two microchannel ports (channel inlet and outlet) with a diameter of 4.00 mm and a poly-dimethylsiloxane (PDMS) thickness of 2.00 mm were used in this study.

The device was composed of a glass slide and a single-layer SU-8 mold based on conventional soft lithography. Briefly, SU-8 5 was first spin-coated on glass, flood exposed, and hard baked to form a seed layer (Figure 2(a)). The mold master was fabricated by spin-coating SU-8 2100/25 on the seed layer with exposure and poste-exposure bake, forming a channel height of 100/20 $\mu$m after development (Figures 2(b) and 2(c)). A 12:1 mixture of PDMS prepolymer and curing agent was thoroughly mixed, poured onto channel masters, degassed under vacuum for air bubble removal, and baked at 80 °C for 3 h (Figure 2(d)). PDMS channels were then removed from the SU-8 masters with ports punched through and bonded to glass slides (Figures 2(e) and 2(f)). The microfluidic devices should be sterilized under UV overnight before used.

### D. Surface coating

Prior to cell-culture experiments, the glass surfaces in microfluidic channels were coated with collagen. Briefly, 1 mg/ml collagen solutions were flushed into the channels through the inlets using micropipets. Then, microfluidic channels were soaked with collagen solutions for 4 h, followed by three-time rinses of supplemented culture medium. The microfluidic devices without collagen coating were used as negative controls by flushing supplemented culture medium into the channels before cell loading.

### E. Cell loading and culture

The cell loading procedure was described in detail in a previous publication, which was summarized briefly as follows.[30] The cells were loaded into microfluidic channels prefilled with supplemented culture medium based on gravity and left 12 h for cell adhesion. Solutions in two ports were removed and replaced with cell suspension solutions at 20 vs. 15 $\mu$l ($0.5 \times 10^6$ cells per ml). Due to the volume difference, cells were pushed into the microfluidic channels due to gravity. Then, each device was placed in a Petri dish containing 2 ml of distilled water and

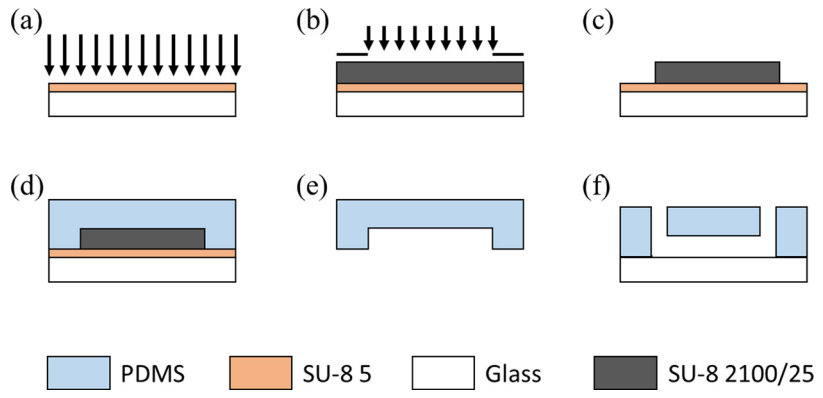


FIG. 2. The microfluidic device fabrication flowchart includes seed layer fabrication based on SU-8 5 (a), channel mold master fabrication using SU-8 2100/25 ((b) and (c)), PDMS channel structure formation ((d) and (e)), and PDMS-glass bonding (f).

transferred to an incubator. Culture medium in each port was replaced with 20 $\mu$l fresh supplemented culture medium every 12 h.

### F. On-chip staining

E11 staining: in the process of on-chip E11 staining, cells within the microfluidic channels were rinsed three times with PBS solutions, fixed by 4% paraformaldehyde in PBS for 10 min at 4 °C, blocked with 10% goat serum/PBS for 45 min at 25 °C. Then, cells were incubated with primary antibodies of 4 $\mu$g/ml overnight at 4 °C, rinsed three times with PBS, incubated with secondary antibodies of 10 $\mu$g/ml for 45 min at 25 °C. Note that in all the steps, solutions of 20 vs. 10 $\mu$l were applied into two ports for medium replacement. The images were taken by an inverted microscope (Olympus IX71).

Live/dead staining: after culturing the osteocytes in the microfluidic channels for 72 h, the viability of osteocytes was assessed by using two specific live/dead probes (e.g., 1 $\mu$g/ml Calcein-AM and 1 $\mu$g/ml propidium iodide). The cells were stained for 10 min at 37 °C, and then washed with PBS for three times, followed by image taken.

Proliferation staining: the on-chip proliferation staining procedure is as follows. Cells within microfluidic devices were washed three times with PBS, fixed by 4% paraformaldehyde in PBS (15 min), permeabilized by 0.5% Triton X-100 (20 min), blocked with 10% goat serum/PBS (1 h). Then, cells within microfluidic devices were incubated with primary antibodies (1:2000) at 4 °C (overnight), secondary antibodies at room temperature (1 h), and the DAB solution with image taken (5 min), sequentially.

Apoptosis staining: to evaluate the osteocyte apoptosis inside microfluidic channels, cells were prefixed by the prefixative solution (fixative:culture medium = 1:1) for 5 min at room temperature. Then, they were fixed by the fixative solution (glacial acetic acid:ethanol = 1:3) for 10 min at room temperature. After washing with PBS three times, the cells were stained by Hoechst 33258 (1 $\mu$g/ml) and incubated at room temperature for 10 min. At the end of the incubation, the cells were washed with PBS for three times, followed by image taken.

### G. Data processing and statistical analysis

To evaluate the osteocyte proliferation and viability inside microfluidic channels, cell numbers and cellular process numbers were counted based on manual processing of phase-contrast images at 12 h, 24 h, 36 h, 48 h, 60 h, and 72 h following cell seeding. All the results were expressed as means ± standard deviations. In the statistical analysis, the Student's t-test was used for two group comparisons. $P < 0.001$ was considered statistically significant.

## III. RESULTS AND DISCUSSION

Previously, MLO-Y4 cells were cultured in a conventional way with well-spread phenotypes and elongated processes.[13,14] This study was designed to investigate the effects of surface coating and channel geometries on phenotypes of MLO-Y4 cells in microfluidic channels. Figure 3 shows microscopic pictures of MLO-Y4 cells seeded in conventional culture dishes (a) and microfluidic channels (b), revealing that MLO-Y4 cells seeded in microfluidic devices demonstrated longer cellular processes and lower cellular body areas compared to conventionally cultured cells. Furthermore, Figure 3(c) shows the microscopic images of immunostaining of E11/gp38 as the benchmark of osteocytes seeded in microfluidic channels, confirming the osteocyte source of MLO-Y4 cells and the feasibility of on-chip osteocyte immunostaining.

### A. Effect of extracellular matrix on MLO-Y4 phenotypes

Previous studies based on conventional cell cultures showed that collagen-coated surfaces can help maintain the osteocyte-like phenotypes of MLO-Y4 cells (e.g., well-spread phenotypes with elongated processes), while MLO-Y4 cells seeded on the non-coated surfaces show a higher proliferation rate.[13,14] This section was designed to investigate the effects of collagen coating on the osteocyte phenotypes expressions in the microfluidic environment.

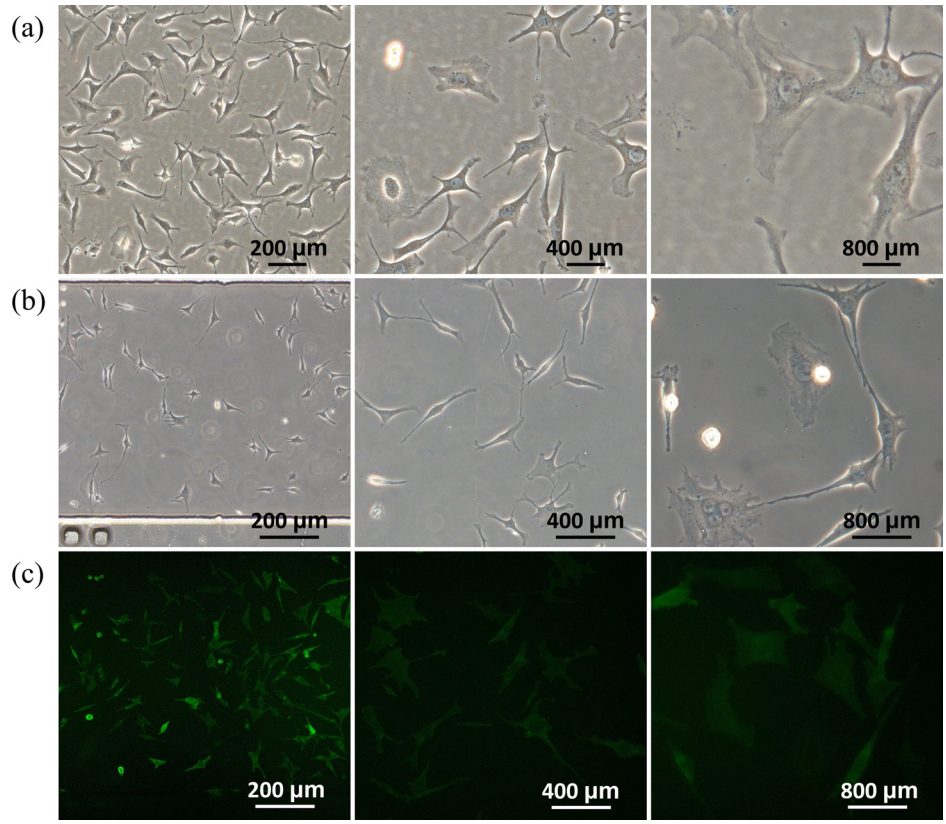


FIG. 3. Microscopic pictures of MLO-Y4 cells seeded in conventional culture dishes (a) and microfluidic channels (b) with on-chip immunostaining of E11/gp38 (c) as the benchmark of osteocytes at 72 h following MLO-Y4 cell seeding (channel dimensions of 10.00 L × 0.80 W × 0.10 H (mm)).

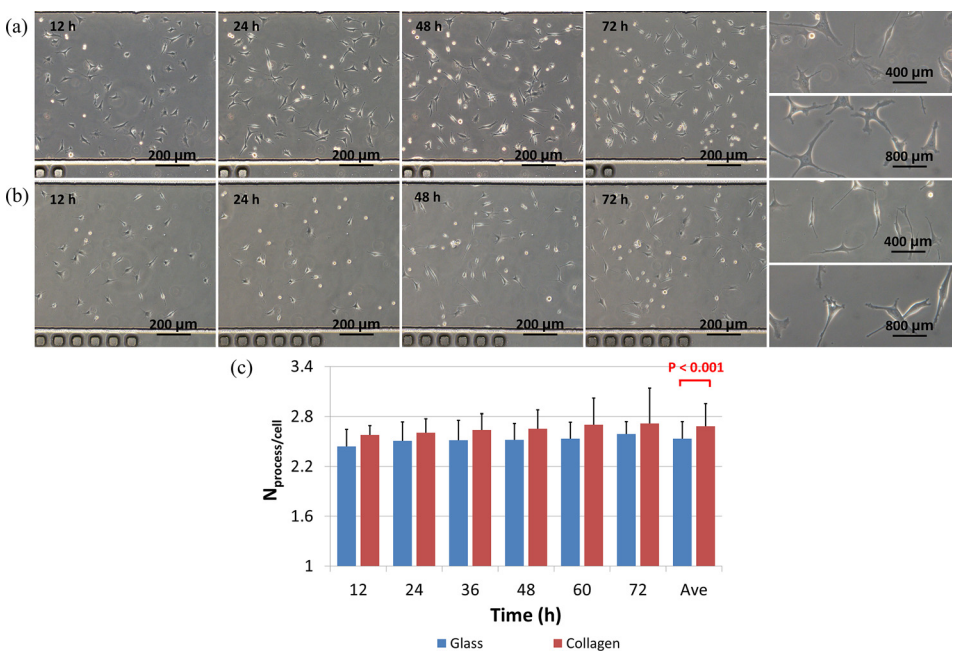


FIG. 4. Time-sequence bright-field microscopic pictures of MLO-Y4 cells seeded in microfluidic channels with (a) and without (b) collagen coating at channel dimensions of 10.00 L × 0.80 W × 0.10 H (mm). (c) Quantified process numbers per cell where a significant difference with and without collagen coating was located.

Figure 4 shows the effects of collagen coating on the morphology of MLO-Y4 cells over time. Within the first 12 h of cell seeding, MLO-Y4 cells on collagen-coated surfaces were shown to spread more (Figure 4(a)) than cells on glass surfaces without collagen coating (Figure 4(b)). As time goes on, elongation in cellular processes and decrease in cell body areas were noticed for both types of surfaces and at 72 h of cell seeding, more processes were located for MLO-Y4 cells on collagen-coated surfaces than cells cultured on bare glass surfaces.

Based on the manual counting, at 72 h following cell seeding, the process number per cell for MLO-Y4 cells cultured on collagen-coated surfaces was quantified as $2.57 \pm 0.11$ (12 h),

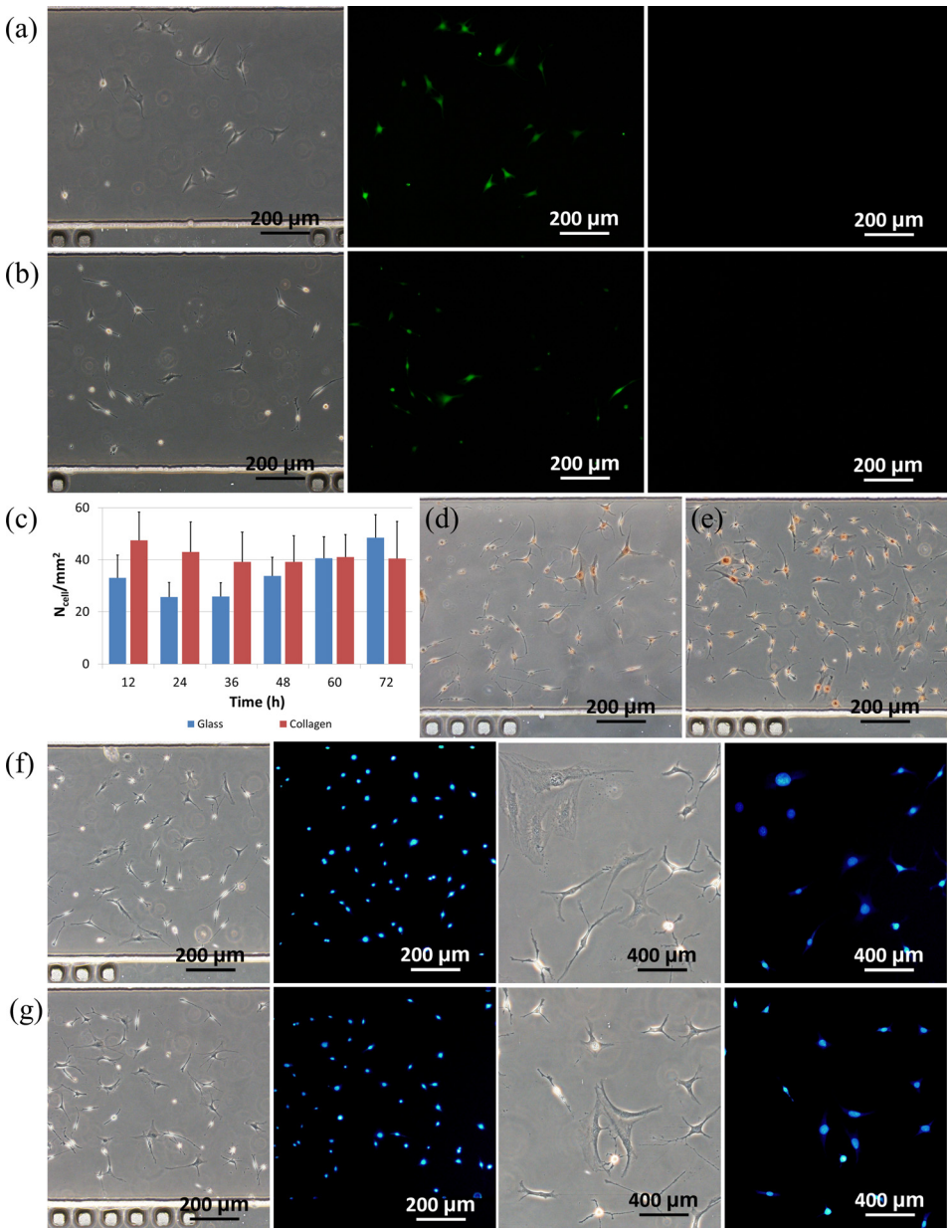


FIG. 5. Microscopic pictures of live/dead staining of MLO-Y4 cells (left: bright field, middle: Calcein-AM staining, and right: propidium iodide staining) seeded in microfluidic channels with (a) and without (b) collagen coating. (c) Compared to MLO-Y4 cells on the glass surfaces, MLO-Y4 cells on the collagen-coated surfaces showed lower proliferation rates. Microscopic pictures of PCNA staining of MLO-Y4 cells seeded in microfluidic channels with (d) and without (e) collagen coating. Microscopic pictures of apoptosis staining of MLO-Y4 cells seeded in microfluidic channels with (f) and without (g) collagen coating. The channel dimensions are 10.00 L × 0.80 W × 0.10 H (mm).

$2.60 \pm 0.17$ (24 h), $2.65 \pm 0.22$ (48 h), $2.70 \pm 0.31$ (60 h) and $2.72 \pm 0.42$ (72 h), while the process number per cell for MLO-Y4 cells seeded on glass surfaces was quantified as $2.44 \pm 0.20$ (12 h), $2.51 \pm 0.23$ (24 h), $2.52 \pm 0.20$ (48 h), $2.53 \pm 0.20$ (60 h) and $2.59 \pm 0.15$ (72 h) (see Figure 4(c)). In summary, a significant difference on cell process number per cell was located as $2.68 \pm 0.27$ vs. $2.53 \pm 0.20$ for MLO-Y4 cells seeded on collagen-coated and glass surfaces, respectively (Figure 4(c)), consistent with the previous studies.[13,14]

As to cellular status, Figures 5(a) and 5(b) show microscopic pictures of live/dead staining of MLO-Y4 cells (left: bright field, middle: Calcein-AM staining and right: propidium iodide staining) seeded in microfluidic channels with (a) and without (b) collagen coating at channel dimensions of 10.00 L × 0.80 W × 0.10 H (mm). These figures record few cells stained with propidium iodide as a confirmation of high cell viability.

As to the cellular proliferation, a similar trend was observed for cells seeded on glass surfaces coated with and without collagen coating in microfluidic channels (see Figure 5(c)). Cell densities on collagen-coated surfaces were quantified as $47.5 \pm 10.8/\text{mm}^2$ (12 h), $43.01 \pm 11.53/\text{mm}^2$ (24 h), $39.13 \pm 10.05/\text{mm}^2$ (48 h), $40.97 \pm 8.66/\text{mm}^2$ (60 h) and $40.41 \pm 14.31/\text{mm}^2$ (72 h), while $32.96 \pm 8.81/\text{mm}^2$ (12 h), $25.58 \pm 5.63/\text{mm}^2$ (24 h), $33.71 \pm 7.15/\text{mm}^2$ (48 h), $40.54 \pm 8.28/\text{mm}^2$ (60 h) and $48.42 \pm 8.91/\text{mm}^2$ (72 h) were quantified values for cells seeded on glass surfaces without collagen coating. For cells seeded in microfluidic channels with and without collagen coating, initial cell density decreases followed by graduate increase in cell numbers were observed. Compared to cells seeded in collagen-coated microfluidic channels, cells seeded on bare glass surfaces were noticed to have a higher proliferation rate.

This trend was confirmed by the PCNA staining result where on non-coated glass surfaces within microfluidic channels, more MLO-Y4 cells were stained with the color of dark yellow compared to the cells on the collagen coated glass surfaces, confirming higher cellular proliferation on non-coated glass surfaces (see Figures 5(d) and 5(e)). These observations of proliferation difference of osteocytes seeded on surfaces with and without collagen coating were consistent with the previous publications.[13,14]

Furthermore, the Hoechst 33258 based apoptosis assay was used to evaluate the cellular apoptosis with and without collagen coating. For MLO-Y4 cells seeded in microfluidic channels with (see Figure 5(f)) and without (see Figure 5(g)) collagen coating, a small portion of cells were stained with a condensed and bright blue color, indicating the initiation of the apoptosis. These results suggested that compared to conventional cell culture, microfluidics based cell culture has limited supply of oxygen and nutrition, providing a less friendly environment for osteocytes.

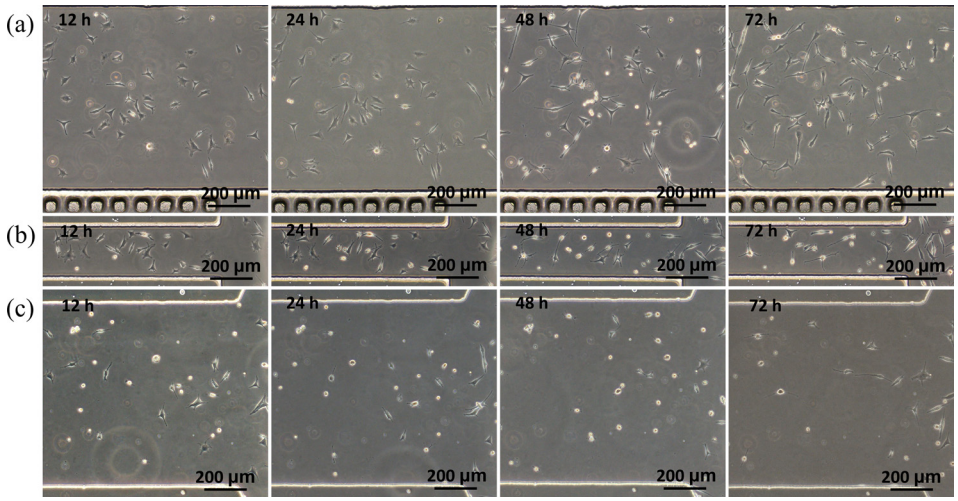


FIG. 6. Time-sequence bright-field microscopic pictures of MLO-Y4 cells cultured in microfluidic channels at dimensions of 10.00 L × 0.80 W × 0.10 H (mm) (a), 10.00 L × 0.20 W × 0.10 H (mm) (b), and 10.00 L × 0.80 W × 0.02 H (mm) (c).

### B. Effect of channel dimensions on MLO-Y4 viability

Channel geometries were located as key parameters affecting cellular viabilities seeded in microfluidic channels[31,32] for a variety of cells. In this study, MLO-Y4 cells were seeded in microfluidic channels with different channel height or width to assess the effect of channel geometries on the cellular viability. Note that in all the experiments, microfluidic channels were

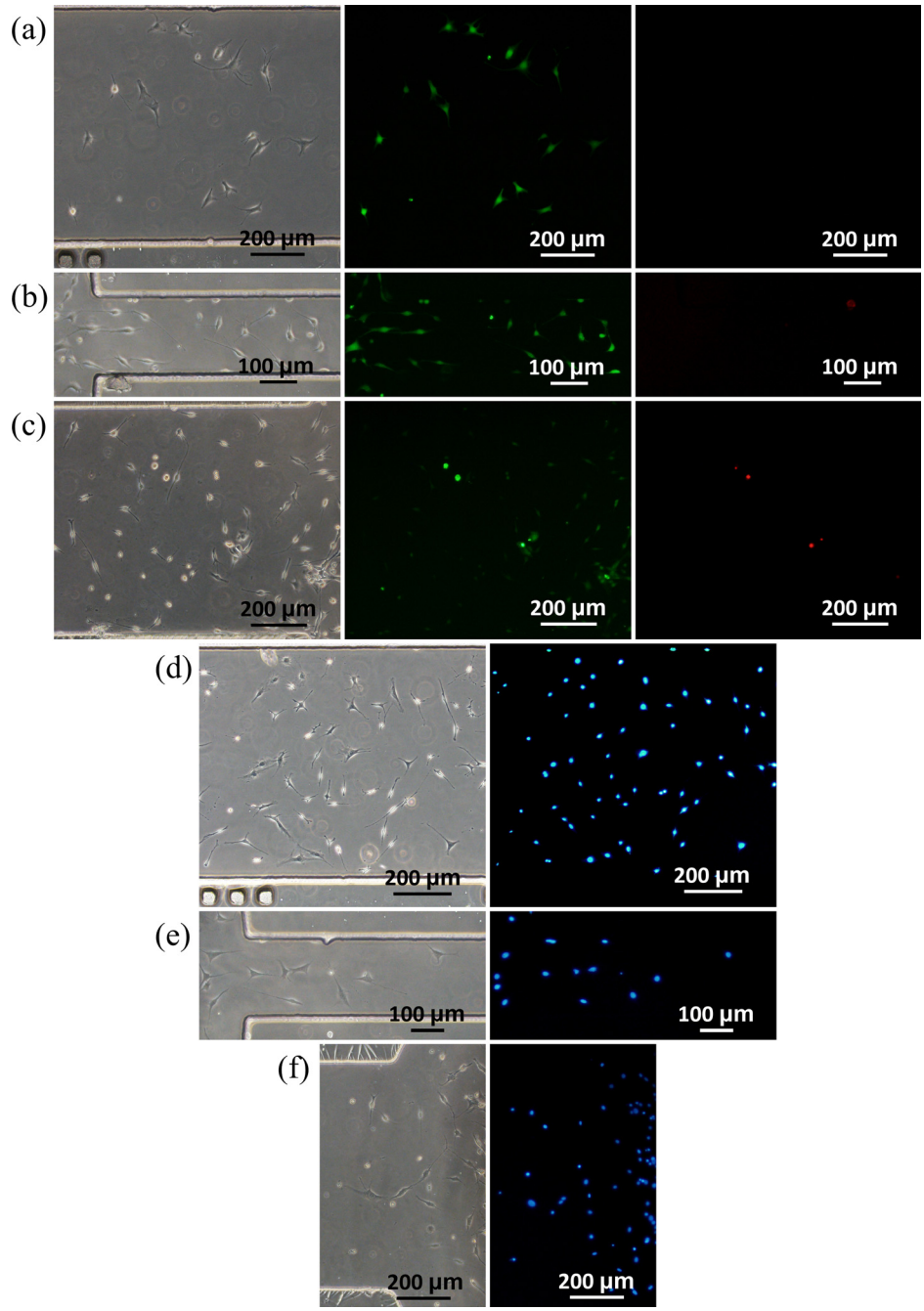


FIG. 7. Microscopic pictures of live/dead staining of MLO-Y4 cells (left: bright field, middle: Calcein-AM staining and right: propidium iodide staining) seeded in microfluidic channels at dimensions of 10.00 L × 0.80 W × 0.10 H (mm) (a), 10.00 L × 0.20 W × 0.10 H (mm) (b), and 10.00 L × 0.80 W × 0.02 H (mm) (c). Microscopic pictures of apoptosis staining of MLO-Y4 cells seeded in microfluidic channels at dimensions of 10.00 L × 0.80 W × 0.10 H (mm) (d), 10.00 L × 0.20 W × 0.10 H (mm) (e), and 10.00 L × 0.80 W × 0.02 H (mm) (f).

coated with collagen as surface modification and the channel length was maintained as 10.00 mm.

As the channel width was decreased from 800 $\mu$m to 200 $\mu$m (channel dimensions of 10.00 L $\times$ 0.20 W $\times$ 0.10 H (mm)), a significant decrease in the cell viability was noticed (Figure 6). At 12 h after cell seeding, MLO-Y4 cells seeded in the middle of the microchannels still maintained the spherical morphology and did not spread on the substrate as a sign of cell death, while cells near the channel inlets were noticed to spread on the substrate and survive well. However, most MLO-Y4 cells near the channel inlets showed elongated cell bodies at 72 h after cell seeding, indicating poor cell status. The same trend was observed for MLO-Y4 cells seeded in microfluidic channels with a decrease of channel height from 100 $\mu$m to 20 $\mu$m (channel dimensions of 10.00 L $\times$ 0.80 W $\times$ 0.02 H (mm)) (Figure 6).

To determine the cell viability in microfluidic channels with different dimensions, staining of Calcein-AM and propidium iodide was conducted (see Figure 7). In channels with decreased width (0.80 vs. 0.20 W (mm), see Figure 7(b)) or height (0.10 vs. 0.02 H (mm), see Figure 7(c)), higher percentages of cells were stained with propidium iodide, suggesting cell death due to the decrease in channel width or height. Note that although more dead cells were located in microfluidic channels with decrease in channel width or height, no significant differences were located in the assay of apoptosis (see Figures 7(d)–7(f)). These differences in cellular viabilities may result from nutrition level distribution, which decreases from the locations near the channel inlets to the middle of the microfluidic channels. This founding was consistent with the previous studies of investigating geometric effects on other types of cells within microfluidic channels.[31,32]

## IV. CONCLUSION

In this paper, a tubing-free microfluidic device was fabricated for MLO-Y4 cell culture where collagen coating, cell seeding, culture and staining were demonstrated. Compared to the glass surfaces, collagen-coated substrates lead to significant differences in MLO-Y4 proliferation and morphology. Microfluidic channels with decreased dimensions were shown to lead to lower viabilities of MLO-Y4 cells due to limited nutrition transportation. As a platform technology, this microfluidic device may function as a new cell culture model enabling further studies of osteocytes.

## ACKNOWLEDGMENTS

The authors would like to acknowledge financial support from National Natural Science Foundation of China (Grant No. 81261120561), National Basic Research Program of China (973 Program, Grant No. 2014CB744600), National Natural Science Foundation of China (Grant No. 61201077), National High Technology Research and Development Program of China (863 Program, Grant No. 2014AA093408), and Beijing NOVA Program.

[1]J. A. Kanis, L. J. Melton III, C. Christiansen, C. C. Johnston, and N. Khaltaev, "The diagnosis of osteoporosis," J. Bone Miner. Res. **9**, 1137–1141 (1994).
[2]J. A. Kanis, "Diagnosis of osteoporosis," Osteoporosis Int. **7**(Suppl. 3), S108–S116 (1997).
[3]A. Mithal and P. Kaur, "Osteoporosis in Asia: A call to action," Curr. Osteoporosis Rep. **10**, 245–247 (2012).
[4]E. Hernlund, A. Svedbom, M. Ivergard, J. Compston, C. Cooper, J. Stenmark *et al.*, "Osteoporosis in the European Union: Medical management, epidemiology and economic burden. A report prepared in collaboration with the International Osteoporosis Foundation (IOF) and the European Federation of Pharmaceutical Industry Associations (EFPIA)," Arch. Osteoporosis **8**, 136 (2013).
[5]M. V. Patel, "Osteoporosis. Endocrinology and metabolism clinics of North America," Ann. Clin. Biochem. **51**, 518–519 (2013).
[6]S. W. Thayer, B. S. Stolshek, G. Gomez Rey, and J. G. Seare, "Impact of osteoporosis on high-cost chronic diseases," Value Health **17**, 43–50 (2014).
[7]G. Bhutani and M. C. Gupta, "Emerging therapies for the treatment of osteoporosis," J. Mid-Life Health **4**, 147–152 (2013).
[8]C. H. Turner and M. R. Forwood, "What role does the osteocyte network play in bone adaptation?," Bone **16**, 283–285 (1995).
[9]T. J. Heino, T. A. Hentunen, and H. K. Vaananen, "Osteocytes inhibit osteoclastic bone resorption through transforming growth factor-beta: Enhancement by estrogen," J. Cell. Biochem. **85**, 185–197 (2002).

[10]L. You, S. Temiyasathit, P. Lee, C. H. Kim, P. Tummala, W. Yao *et al*., "Osteocytes as mechanosensors in the inhibition of bone resorption due to mechanical loading," Bone **42**, 172–179 (2008).
[11]M. B. Schaffler and O. D. Kennedy, "Osteocyte signaling in bone," Curr. Osteoporosis Rep. **10**, 118–125 (2012).
[12]C. A. O'Brien, T. Nakashima, and H. Takayanagi, "Osteocyte control of osteoclastogenesis," Bone **54**, 258–263 (2013).
[13]Y. Kato, J. J. Windle, B. A. Koop, G. R. Mundy, and L. F. Bonewald, "Establishment of an osteocyte-like cell line, MLO-Y4," J. Bone Miner. Res. **12**, 2014–2023 (1997).
[14]L. F. Bonewald, "Establishment and characterization of an osteocyte-like cell line, MLO-Y4," J. Bone Miner. Metab. **17**, 61–65 (1999).
[15]I. Kalajzic, B. G. Matthews, E. Torreggiani, M. A. Harris, P. Divieti Pajevic, and S. E. Harris, "*In vitro* and *in vivo* approaches to study osteocyte biology," Bone **54**, 296–306 (2013).
[16]G. M. Whitesides, "The origins and the future of microfluidics," Nature **442**, 368–373 (2006).
[17]R. C. Wootton and A. J. Demello, "Microfluidics: Exploiting elephants in the room," Nature **464**, 839–840 (2010).
[18]E. K. Sackmann, A. L. Fulton, and D. J. Beebe, "The present and future role of microfluidics in biomedical research," Nature **507**, 181–189 (2014).
[19]E. W. Young and D. J. Beebe, "Fundamentals of microfluidic cell culture in controlled microenvironments," Chem. Soc. Rev. **39**, 1036–1048 (2010).
[20]I. Meyvantsson and D. J. Beebe, "Cell culture models in microfluidic systems," Annu. Rev. Anal. Chem. **1**, 423–449 (2008).
[21]H. Ma, H. Xu, and J. Qin, "Biomimetic tumor microenvironment on a microfluidic platform," Biomicrofluidics **7**, 11501 (2013).
[22]D. Wlodkowic and J. M. Cooper, "Tumors on chips: Oncology meets microfluidics," Curr. Opin. Genet. Dev. **14**, 556–567 (2010).
[23]A. K. Soe, S. Nahavandi, and K. Khoshmanesh, "Neuroscience goes on a chip," Biosens. Bioelectron. **35**, 1–13 (2012).
[24]K. H. Wong, J. M. Chan, R. D. Kamm, and J. Tien, "Microfluidic models of vascular functions," Annu. Rev. Biomed. Eng. **14**, 205–230 (2012).
[25]A. D. van der Meer, A. A. Poot, M. H. Duits, J. Feijen, and I. Vermes, "Microfluidic technology in vascular research," J. Biomed. Biotechnol. **2009**, 823148.
[26]M. E. Hasenbein, T. T. Andersen, and R. Bizios, "Micropatterned surfaces modified with select peptides promote exclusive interactions with osteoblasts," Biomaterials **23**, 3937–3942 (2002).
[27]S. Lenhert, M. B. Meier, U. Meyer, L. Chi, and H. P. Wiesmann, "Osteoblast alignment, elongation and migration on grooved polystyrene surfaces patterned by Langmuir-Blodgett lithography," Biomaterials **26**, 563–570 (2005).
[28]S. Kou, L. Pan, D. van Noort, G. Meng, X. Wu, H. Sun *et al*., "A multishear microfluidic device for quantitative analysis of calcium dynamics in osteoblasts," Biochem. Biophys. Res. Commun. **408**, 350–355 (2011).
[29]J.-H. Lee, Y. Gu, H. Wang, and W. Y. Lee, "Microfluidic 3D bone tissue model for high-throughput evaluation of wound-healing and infection-preventing biomaterials," Biomaterials **33**, 999–1006 (2012).
[30]Y. C. Wei, F. Chen, T. Zhang, D. Y. Chen, X. Jia, J. B. Wang *et al*., "Vascular smooth muscle cell culture in microfluidic devices," Biomicrofluidics **8**, 046504 (2014).
[31]E. Leclerc, Y. Sakai, and T. Fujii, "Cell culture in 3-dimensional microfluidic structure of PDMS (polydimethylsiloxane)," Biomed. Microdevices **5**, 109–114 (2003).
[32]H. Yu, I. Meyvantsson, I. A. Shkel, and D. J. Beebe, "Diffusion dependent cell behavior in microenvironments," Lab Chip **5**, 1089–1095 (2005).